catalysts

MDPI

Article

Nature and Location of Carbonaceous Species in a Composite HZSM-5 Zeolite Catalyst during the Conversion of Dimethyl Ether into Light Olefins

María Ibáñez, Paula Pérez-Uriarte, Miguel Sánchez-Contador, Tomás Cordero-Lanzac, Andrés T. Aguayo, Javier Bilbao and Pedro Castaño *

Department of Chemical Engineering, University of the Basque Country (UPV/EHU), P.O. Box 644, 48080 Bilbao, Spain; maria.ibanez@ehu.eus (M.I.); paula.perez@ehu.eus (P.P.-U.); miguel.sanchezcontador@ehu.eus (M.S.-C.); tomas.cordero@ehu.eus (T.C.-L.); andrestomas.aguayo@ehu.eus (A.T.A.); javier.bilbaoe@ehu.eus (J.B.)
* Correspondence: pedro.castano@ehu.eus; Tel.: +34-94601-8435

Academic Editor: Rafael Luque
Received: 18 July 2017; Accepted: 25 August 2017; Published: 30 August 2017

Abstract: The deactivation of a composite catalyst based on HZSM-5 zeolite (agglomerated in a matrix using boehmite as a binder) has been studied during the transformation of dimethyl ether into light olefins. The location of the trapped/retained species (on the zeolite or on the matrix) has been analyzed by comparing the properties of the fresh and deactivated catalyst after runs at different temperatures, while the nature of those species has been studied using different spectroscopic and thermogravimetric techniques. The reaction occurs on the strongest acid sites of the zeolite micropores through olefins and alkyl-benzenes as intermediates. These species also condensate into bulkier structures (polyaromatics named as coke), particularly at higher temperatures and within the meso- and macropores of the matrix. The critical roles of the matrix and water in the reaction medium have been proved: both attenuating the effect of coke deposition.

Keywords: ZSM-5 (MFI) zeolite; dimethyl ether (DME); light olefins; propylene; coke

1. Introduction

The chemical industry needs non-conventional processes to be developed, that are environmentally friendly and based on renewable sources, to meet the growing demand for fuels and chemicals. In this scenario, the production of light olefins (in particular of propylene) receives great attention [1,2] due to the increasing demand for its derivatives: polypropylene, propylene oxide and acrylonitrile. Although the current production of light olefins is based on naphtha steam cracking, the high energy requirement of this process (with high CO_2 emissions) and its reduced selectivity of propylene explain the interest of other processes [3]. In this way, the increasing industrial implantation of the MTO (methanol to olefins) process [4] offers the possibility of obtaining methanol from different fossil sources alternative to petroleum (carbon, natural gas) and also from biomass (via gasification). Alternatively, the DTO (dimethyl ether to olefins) process has some important advantages. Firstly, the synthesis of dimethyl ether (DME) is thermodynamically more favorable than that of methanol [5], which allows it to operate at higher temperature, lower pressure, and using a lower H_2/CO ratio (facilitating the use of biomass syngas). This weakened thermodynamic limitation also favors the enhancement of CO_2 co-fed with the syngas [5,6]. Secondly, reactor operability is simpler in the DTO process than in the MTO due to the elimination of the exothermic step of methanol dehydration [7]. These benefits have motivated the Lurgi process (dehydration of methanol and on-line conversion of the product stream to light olefins) [8].

The HZSM-5 zeolite catalyst shows outstanding activity and selectivity in the DTO conversion (as in the second stage of the Lurgi process), with greater stability than those of SAPO-18 and -34 catalysts [9–13]. The performance of high-silica HZSM-5 zeolite reaches a compromise between the light olefin selectivity, and an extended catalyst lifetime [14]. This behavior has been associated with its unique acid and textural properties [15–18]. In this sense, HZSM-5 zeolite displays acid sites of relatively weak strength nature and a three-dimensional porous network with two groups of interconnected channels: ellipsoidal 5.3 × 5.6 Å and sinusoidal 5.1 × 5.5 Å and without cages at intersections. In this type of zeolites and zeotypes, DTO mechanism is assumed to occur through the "dual cycle mechanism" (similar to MTO), with olefins and arenes (alkyl-benzenes) being the intermediates in the oligomerization-cracking and olefin/aromatic methylation-dealkylation routes [19]. The pore topology of HZSM-5 zeolite makes the arene cycle particularly dominating for highly acid catalysts [20]. Regarding the arene cycle, the species involved decrease their DTO activity when they are highly methylated or alkylated [21].

For the industrial implementation of the DTO process, with a technology similar to that of the MTO process [22] (interconnected bubbling fluidized bed reactor and regenerator), the attrition problem of the HZSM-5 must be solved [23]. For this reason, zeolite is agglomerated within a matrix that provides the catalyst particles with the appropriate mechanical and physical properties. Furthermore, the matrix provides the microporous zeolite with an additional system of meso- and macropores [24]. Michels et al. [25] highlight the importance of the zeolite agglomeration in order to use the catalyst at industrial scale, yielding a final catalyst composite with an improved mechanical resistance and a hierarchical porous texture that extends the catalyst lifetime. Indeed, the catalyst lifetime is a crucial point for enhancing the global competitiveness of the DTO process, and this feature lies in the formation of coke [26]. Coke is formed through a combination of pathways from precursors that have an olefinic, and mainly, an aromatic nature [27]. Thus, the same alkyl-benzenes lead to the formation of light olefins and coke [28,29]. Previous works about DTO conversion show the impact of different catalytic features in controlling the catalyst deactivation, and among them (for a given zeolite), the zeolite agglomeration with boehmite as binder [15], obtaining a proper spatial distribution in the matrix [30], attenuates the deactivation by coke. This effect has been observed in other reactions using a HZSM-5 catalyst, explaining that the deposition of coke on the meso- and macropores of the matrix delays the blockage of the micropore mouths of the zeolite [31].

The aim of this work is to analyze the species present on a composite catalyst (high-silica HZSM-5 zeolite agglomerated with boehmite as a binder) during the DTO conversion. A comparison of the properties of the fresh with the deactivated catalysts (in the temperature range of 325–375 °C), on the grounds of the results of N_2 and tert-butylamine (t-BA) adsorption-desorption, has enabled us to locate the carbonaceous species deposited on the zeolite and matrix surface. Different techniques have been used in order to separately characterize the coke precursors, which are also intermediates in the formation of olefins (TPD analysis in N_2), and the coke itself (TPO analysis). Both carbonaceous species have been also characterized through FTIR-TPO and UV-vis spectroscopic experiments.

2. Results and Discussion

2.1. Evolution of Conversion and Selectivity

Figure 1a shows the evolution of DME conversion over time on stream at 325, 350 and 375 °C. These results indicate the presence of two stages of deactivation at 325–350 °C: a faster one (325 °C, 0–1 h; 350 °C, 0–2 h) and a slower one, which leads to a steady conversion value at those temperatures. A single deactivation stage is observed at 375 °C due to the even faster first stage of deactivation. Within the given time on stream range studied, the deactivation is faster as the temperature is increased from 325 to 350 °C (observing a conversion drop of 50% and 61%, respectively). However, at 375 °C, the conversion only drops 19% of the initial one. All these stages have been previously associated to the sequenced deactivation of the strongest (fast deactivation step: at 375 °C the reaction is so fast

that cannot be observed) and weakest (slow deactivation step) acid sites. The products obtained have been classified into methanol, light olefins, C_{5+} aliphatics (from where more than 90% correspond to C_{5+} olefins), paraffins, aromatics and coke. From the industrial perspective, C_{5+} aliphatics and some paraffins, as butane, could be recirculated for boosting olefin production and controlling coke deactivation [32]. Figure 1b shows the values of selectivity of light olefins at different temperatures for time on stream values of 0 and 18 h. As the temperature is increased, the selectivity of olefins decreases due to the faster secondary reactions of those: (i) oligomerization-cracking, leading to C_{5+} aliphatics; (ii) hydrogen transfer, leading to paraffins and aromatics; and (iii) condensation, leading to coke. An increase in the selectivity of olefins is observed when the catalyst is partially deactivated after 18 h, which suggests that light olefins are midway compounds within the reaction network. In this regard, deactivation affects more severely the secondary reactions of light olefins compared with the primary formation ones, corresponding to hydrocarbon dual cycle mechanism. This kind of behavior is clearer when the temperature is raised (+3% at 325 °C and +21% at 375 °C), which has been also reported in the transformation of ethanol into hydrocarbons [33] and the catalytic cracking of vacuum gas oil [34].

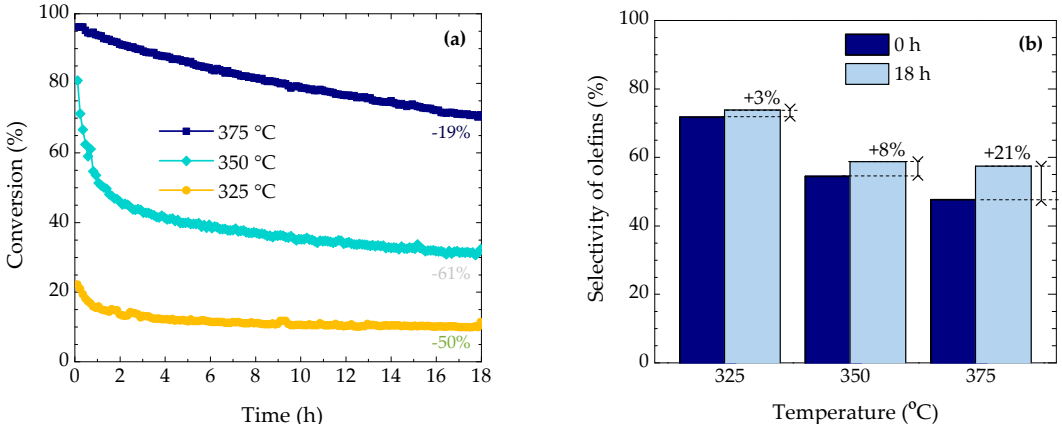

Figure 1. (**a**) Effect of reaction temperature on the evolution of DME conversion with time on stream and its relative decrease after 18 h. (**b**) Selectivity of olefins at 0 and 18 h at 325, 350 and 375 °C. Annotations refer to (**a**) the decrease in the DME conversion values and (**b**) the increase in the selectivity values.

2.2. Location of Coke

Figure 2 shows the effect of the γ-Al_2O_3 matrix on the textural and acid properties, while also the deterioration of those after reactions at different temperatures. As is observed in Figure 2a, the HZSM-5 zeolite exhibits a N_2 adsorption-desorption isotherm typical of microporous materials, adsorbing the majority of N_2 at very low relative pressures. In contrast, the γ-Al_2O_3 matrix (as the product of boehmite calcination) displays a type IV isotherm, with main adsorption step at relative pressures higher than 0.4 (in the range of mesoporous). Regarding the isotherm of the agglomerated catalyst, a decrease in the N_2 adsorption at low relative pressure can be observed compared with the bare zeolite as a consequence of the presence of the matrix, which makes a "dilution effect" of the zeolite micropores. However, a wide range of relative pressure for N_2 adsorption is shown by the catalyst, which suggests that the matrix provides the final catalyst with a mesoporous texture additional to that of the zeolite crystals. The values of S_{BET} for the zeolite and the matrix are 441 and 120 $m^2 \cdot g^{-1}$, whereas the final catalyst displays a S_{BET} of 315 $m^2 \cdot g^{-1}$. Likewise, a modification on the acid properties is exhibited by the catalyst after its agglomeration. Figure 2b shows the TPD-cracking profile of t-BA for the HZSM-5 zeolite and for the agglomerated catalyst, which have been previously reported [15]. It is worthy of remarking that the lower the temperature of the peak, the stronger the acid site, since the temperature needed for t-BA cracking is lower. In such a way, the TPD-cracking

profile of t-BA for HZSM-5 catalyst shows two defined peaks related to strong and weak acid sites (208 and 260 °C, respectively) and the γ-Al_2O_3 matrix only shows one peak attributed to acid sites even weaker than those of the zeolite (275 °C). The total acidity of the matrix is insufficiently active for the DTO conversion. This was proven in a reaction using only the matrix without a catalyst, where low DME conversion was observed, only yielding CO and CH_4 (as the products of the thermal cracking of DME). The final catalyst shows a well-defined peak at 232 °C (not as strong as that of the zeolite, appearing at 208 °C) and a second broad peak at ca. 250–350 °C that corresponds to the weak acid sites of the γ-Al_2O_3 matrix [15]. The shift of the peak attributed to the strong acid sites can be associated with the partial covering of the zeolite crystals by the matrix, thus hindering the adsorption of the t-BA on the strongest acid sites located on the external surface of the crystals.

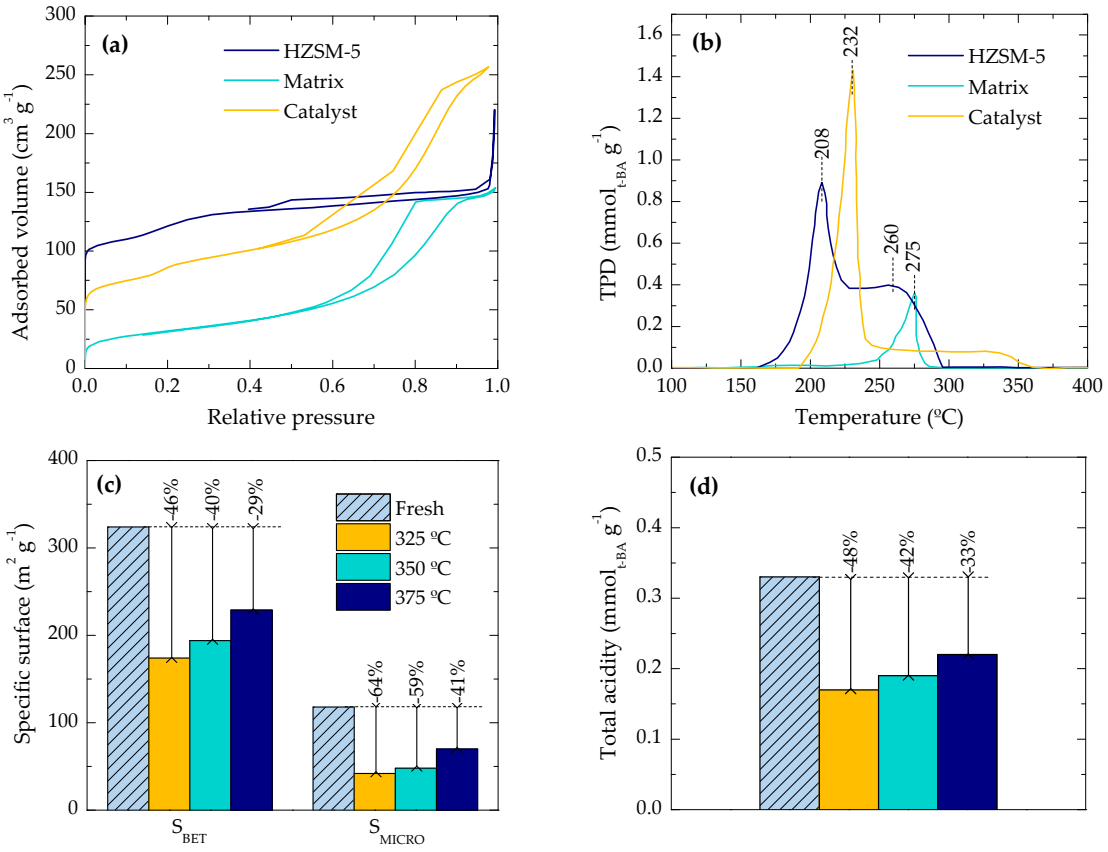

Figure 2. (**a**) N_2 adsorption-desorption isotherms and (**b**) t-BA desorption profiles of the HZSM-5 zeolite, the γ-Al_2O_3 matrix and the final catalyst. Effect of reaction temperature on the deterioration of (**c**) the specific BET surface area and the micropore surface area, and (**d**) the total acidity of deactivated catalysts (annotations refer to the decrease in each value).

The deterioration of the textural properties of the catalyst is shown in Figure 2c, whereas Figure 2d displays the drop of the total acidity of the catalyst during the reaction (area below TPD-cracking profile). As concluded from the results of Figure 2a, the micropores of the catalyst are mainly provided by the HZSM-5 zeolite crystals and thus, the decrease in the microporous specific surface area (S_{MICRO}) is evaluated together with the one in the BET specific surface area (S_{BET}). The S_{BET} drop is severer at lower reaction temperatures (Figure 2c), and this trend is even more pronounced for the S_{MICRO}. This indicates a parallel deposition of carbonaceous species in the zeolite (micropores) and the matrix (meso- and macropores). Comparing with the previous results (Figure 1), the slower deactivation at lower temperature (325 °C) is correlated with a higher degradation of the S_{MICRO}, which is associated with species trapped in the zeolite micropores. On the other hand, the apparently discrepant result of

less deactivation and deterioration of S_{MICRO} at higher temperature (375 °C) can be explained by the preferential deposition of coke in the meso- and macropores of the matrix, causing the blockage of the micropore mouths of the zeolite. These results are consistent with those reported by Schulz et al. [28] for the conversion of methanol. Their results reveal a preferential coke deposition within the micropores of the zeolite HZSM-5 below 350 °C, and an evolution of the external coke above this temperature. The formation of external coke is commonly associated with the diffusion of the coke precursors outside the HZSM-5 zeolite crystals, increasing the amount of external coke with the catalyst deactivation state [35–37].

The TPD-cracking of t-BA for the deactivated catalyst shows a peak shift of −3 °C (Figure not shown), which suggests that coke blocks preferentially the strongest acid sites, attenuating their capacity of adsorption and cracking of t-BA. Figure 2d illustrates the decay in the total acidity of the catalyst deactivated at different temperatures. The increase of the total acidity upon increasing the reaction temperature is in agreement with the trend observed for S_{MICRO} (Figure 2c), and it is also consistent with our previous hypothesis: HZSM-5 zeolite provides the final catalyst with the microporous texture and the acidity. This result can be related to the composition of the reaction medium, because the concentration of aromatics and steam also increase with temperature. The role of steam in the attenuation of coke precursor formation and in the promotion of their diffusion outside the zeolite channels is well established in the literature [38–40]. The three-dimensional micropores of the HZSM-5, with a high number of intersections and without cages, is the suitable pore network in order to favor this diffusion. However, the larger pore size of the matrix allows the growth of the coke precursors to polyaromatic structures, decreasing the blockage of the micropore mouths of the zeolite. This is one of the main advantages of using the matrix-containing catalyst compared to the matrix-free zeolite, as we previously reported in detail [15].

2.3. Coke Nature

Table 1 shows the amount of carbonaceous species retained in the deactivated catalyst that are desorbed in the temperature programmed desorption with N_2 (TPD species) or combusted in the temperature programmed oxidation (TPO species or coke). The profiles of desorption and oxidation (in sequenced manner) are shown in Figure 3. TPD species are associated with certain intermediate compounds in the reaction or in the formation of coke mechanisms [41,42]. On the other hand, coke species are the ones retained in the catalyst after the TPD experiment, and therefore they are considered as the coke that causes the catalyst deactivation. As the DTO temperature is increased, the amount of TPD species decreases due to the unfavorable adsorption equilibrium. However, the amount of coke deposited during the reaction increases upon increasing the reaction temperature. This, together with the lower deterioration of the catalytic properties at higher temperatures, indicates the preferential deposition of coke on the meso- and macropores of the catalyst (associated with the matrix) at this condition. Nevertheless, the higher degradation of the textural and acid properties at lower reaction temperatures is consistent with the higher total amounts of carbonaceous species (TPD species and coke, 4.98 wt % and 3.99 wt % at 325 and 375 °C, respectively).

Table 1. Amounts of carbonaceous species deposited on the catalyst during the reaction determined by means of TPD and TPO analyses.

Temperature (°C)	325	350	375
TPD Species (wt %)	3.64	3.33	2.57
Coke (wt %)	1.33	1.41	1.42
Total (wt %)	4.98	4.75	3.99

The TPD profiles (under N_2 flux, Figure 3a) show two desorption peaks tentatively associated with the aging (dehydrogenation) of coke or the desorption of intermediates (olefins and alkyl-aromatics). The intensity of the first peak decreases when the reaction temperature is increased, which suggests

that the H/C ratio of coke decreases at higher temperatures [43]. Otherwise, TPO profiles (Figure 3b) show a main combustion peak at 550 °C and a shoulder (at higher DTO temperatures) at 450 °C. The TPO peak with maximum at 450 °C can be associated with aliphatic coke deposited on the meso- and macropores of the matrix [36,44], whereas the peak with a maximum at 550 °C can be attributed to the combustion of condensed aromatics (polyaromatics) of coke in the micropores or heavy structures in the meso- and macropores. In a previous work, we proved that the deposition of aliphatic coke is less selective, and also occurs in the matrix material [31].

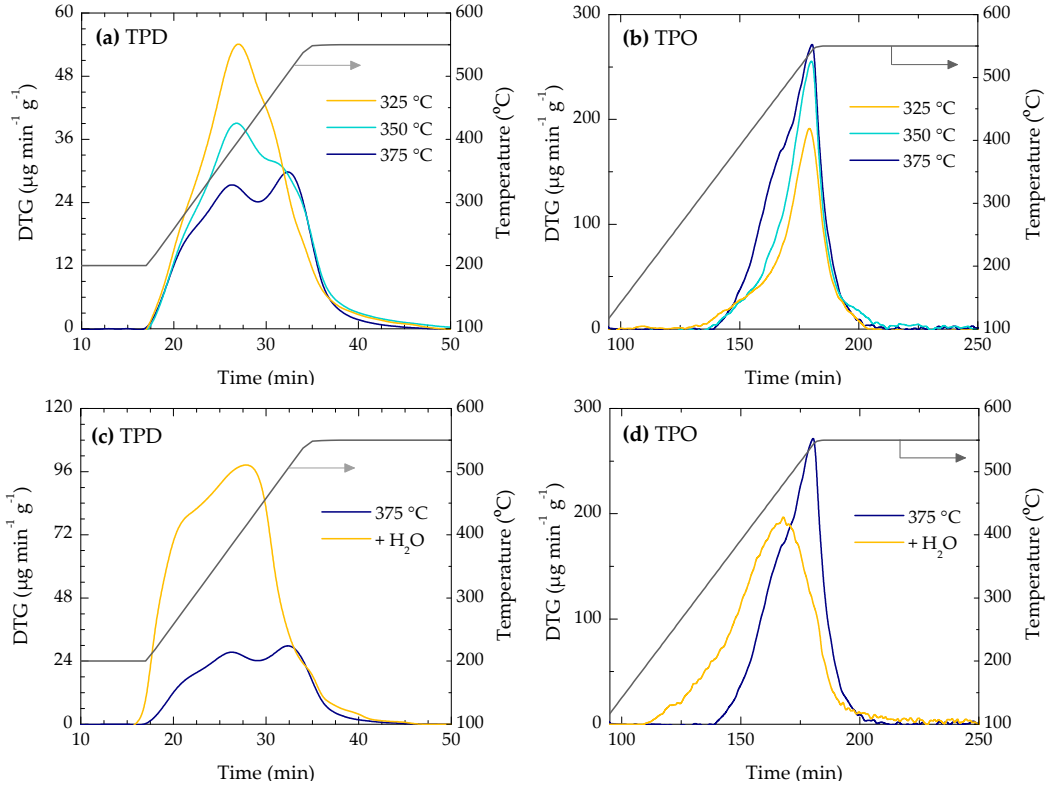

Figure 3. (**a**) TPD profiles under N_2 flow and (**b**) TPO profiles of deactivated catalysts at 325, 350 and 375 °C. Effect of co-feeding water on the (**c**) TPD and (**d**) TPO profiles of the deactivated catalyst at 375 °C.

An important factor in the catalyst deactivation is the higher concentration of water in the reaction medium at higher temperatures [45]. It is well established that the effect of water (steam) to attenuate coke deposition in the MTO process and in general in the transformation of oxygenates into hydrocarbons [38–40], which is attributed to different possible causes: (i) competitive adsorption on acid sites with coke precursors; (ii) attenuation of the acid strength of the sites; (iii) attenuation of the formation of methyloxonium ions (initial adsorbed reagents) in equilibrium with both methanol and DME in the reaction medium, and whose equilibrium is displaced by water; (iv) formation of phenols from aromatic (precursors of coke) activated by acid sites [46]; (v) the entrainment by the water molecules of coke of catalytic origin and which are retained in the crystalline channels. In this regard, the previous results suggest that water favors the shift of coke precursors from the micro- to the meso- and macropores of the catalyst. Nevertheless, the presence of water also has a negative effect, as the reaction rate of olefin production is reduced [47], according to the first three hypotheses above described [38–40]. Hence, these opposed effects must be considered for the reactor design in order to optimize the co-feeding of water.

In order to clarify these issues, a reaction in which water was co-fed with DME was carried out. Figure 3c,d show the TPD and TPO profiles, respectively, for the deactivated catalyst at 375 °C.

The TPD profile (under a N_2 flux) of the catalyst shifts toward lower temperatures, which suggests an increase in the H/C ratio of the retained carbonaceous species when the amount of steam in the reaction medium is increased. This result, together with the maximum observed at ca. 440 °C in the TPO profile (Figure 3d), points to a more aliphatic nature of the coke when co-feeding water. Moreover, a widening of the TPO profile occurs for the combustion of the coke deposited during the DTO reaction with water. This indicates that the nature of this coke is more heterogeneous than those of the coke illustrated in Figure 3b. On the other hand, the attenuation of the peak at 550 °C (previously attributed to the coke deposited on the zeolite) confirms that the steam sweeps the precursor of coke to the external mesopores of the matrix. In such a way, the combustion of this coke occurs at a lower temperature (440 °C) and the deactivation of the catalyst is attenuated. These results are consistent with the previously reported ones [22,34–37].

The FTIR-TPO and UV-vis analyses have been carried out in order to obtain more compositional insights of the carbonaceous species deposited on the catalyst surface during the DTO conversion. Figure 4a shows the results of FTIR-TPO profiles, determined in a single run, of the species deposited on the catalyst at 325 °C. The MS spectrometry has been used to track the CO_2 signal and the FTIR spectroscopy has been used to analyze the derivative of absorbance bands (dA/dt) of four groups of species trapped on the catalyst [48–50]: $–CH_3$ at 2960 cm^{-1}; $–CH_2$ and –CH at 2930 cm^{-1}; conjugated double bonds in dienes or aromatics at 1610 cm^{-1}; condensed aromatics at 1580 cm^{-1}.

The profile of MS-TPO show a very broad peak, which comprises the previously named TPD species and coke. The evolution of the dA/dt (FTIR-TPO) indicates three sequenced stages of reaction: (1) dehydrogenation of paraffinic bounds at temperature lower than 300 °C forming dienes and aromatics, (2) combustion of aliphatic coke at 340–380 °C, and (3) combustion of condensed aromatic coke at 480 °C. The divergence of temperature values between TG-TPO and FTIR-TPO analyses are due to the coke aging during the TPD (performed prior the TG-TPO) and thus, the combustion peaks in the former technique appear at higher temperatures [51]. The results of the FTIR spectroscopy show that the effect of temperature on the coke composition is not relevant, so additional analyses are required. Besides, the same trend of lower deposition of carbonaceous species when the DTO temperature is raised is observed (less intensity of MS-TPO signals are observed for the catalyst deactivated at 350 and 375 °C compared with that of Figure 4a).

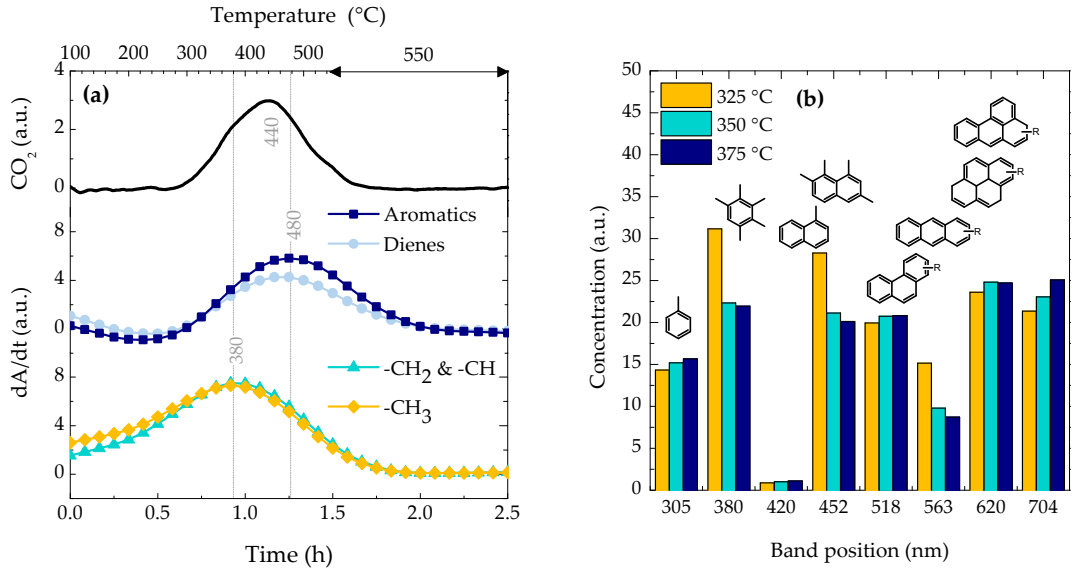

Figure 4. (**a**) Evolution of the CO_2 signal (MS) and the composition of the carbonaceous species remained in the solid (by means of FTIR spectroscopic bands) during the TPO experiment of the deactivated catalyst at 325 °C. (**b**) Concentration of the carbonaceous species trapped inside the deactivated catalyst (by means of UV-vis spectroscopy) at 325, 350 and 375 °C.

On the other hand, each of the UV-vis spectrum of the deactivated catalysts has been deconvoluted in 8 Gaussian peaks with increasing number of aromatic rings [52,53]: 305 nm, low alkylated one ring aromatics (alkyl-benzenes); 380 nm, high alkylated one ring aromatics (polyalkyl-benzenes); 420–452 nm, low and high alkylated naphthalenes and biphenyls; 518–564 nm, low and high alkylated phenanthrenes and anthracenes; and 620–704 nm, more condensed aromatic structures such as alkylated pyrene and aromatics with more than 5 rings. Figure 4b shows the results of the deconvolution of the UV-vis spectra for the deactivated catalyst at different temperatures. The presence of alkyl-benzenes and polyaromatics (particularly 5+ ring aromatics) increases with the increase of temperature.

As discussed in the introduction, the dual cycle mechanism involves two distinctive species (olefins or aromatics), whose predominance is still under strong debate. The group of Bhan [19,20] has proposed different selectivity ratios in order to quiantify the importance of each cycle, e.g., the ethylene/isobutane ratio is representative of the arene/olefin cycle ratio [19]. Thus, Figure 5 displays the values of ethylene/isobutane ratio at different temperatures for time on stream values of 0 and 18 h. As observed, the arene cycle dominates at lower temperatures and longer time on stream values. Thus, the results of Figure 4b or Figure 5 indicates that the presence of alkyl-benzenes is linked with the DME conversion observed in Figure 1a, while the higher concentration of 5+ ring aromatics is responsible of the higher amount of coke observed in Table 1. According to Section 2.2, these alkyl-benzenes are located close to the acid site of the zeolite and within its micropores.

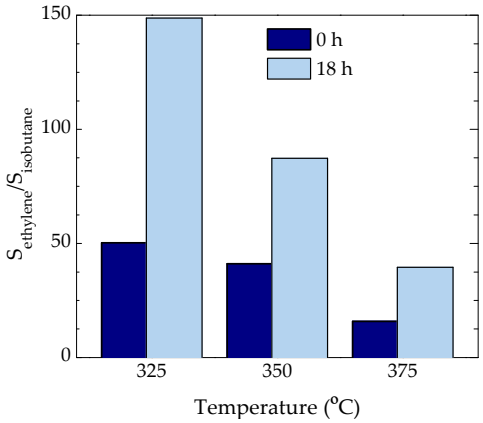

Figure 5. Effect of reaction temperature and time on stream (0 and 18 h) on the ethylene/isobutane selectivity ratio (referred to C units).

The hereby presented results propose that the mechanism of DME conversion into light olefins on HZSM-5 zeolite follows the dual cycle mechanism dominated by the aromatic cycle. The relatively low acidity and acid strength (due to its low aluminum concentration) of the used zeolite hampers the parallel-sequenced reactions of oligomerization-cracking, hydrogen transfer and condensation, leading to relatively high olefin selectivity. At 325 °C the aromatic cycle is dominated by polyalkyl-benzenes (of lower activity than alkyl-benzenes) leading to a lower DME conversion but a higher olefin selectivity. These species are located within the micropores of the catalyst in close proximity to the strongest acid sites. The strongest acid sites, which are the most active ones for condensing the alkyl-benzene species, are blocked by coke at initial time on stream values. On the other hand, the sites with moderate acid strength remain active for longer and do not promote the condensation of these species as fast as the strongest ones. As the temperature is increased (up to 375 °C), the presence of alkyl-benzenes is higher, leading to a higher DME conversion and a lower olefin selectivity, as a consequence of the greater advance of the reaction when increasing the temperature. The higher concentration of water in the reaction medium at higher temperature favors the expulsion of coke precursors toward the meso- and macropores of the matrix, where they are transformed into bulky polyaromatics. The presence

of the matrix attenuates the deactivating effect of these polyaromatics, whose deposition blocks the micropore mouths of the zeolite.

3. Materials and Methods

3.1. Catalysis Preparation

The catalyst used in the reactor has been prepared by agglomerating 50 wt % of active phase (zeolite with SiO_2/Al_2O_3 ratio 280 supplied by Zeolyst International, Conshohocken, PA, USA) with 30 wt % of binder (boehmite, 77 wt %, Sasol, Hamburg, Germany) and a 20 wt % of inert-filler material (colloidal alumina, 20 wt %, Alfa Aesar, Haverhill, MA, USA). This catalyst agglomeration is required because a fast deactivation and a break of the particles are observed in the experiments with pure zeolite. This deactivation and the zeolite particles fragility avoid the reutilization of the catalyst through combustion of coke. Thus, the catalyst particles have been obtained by wet extrusion method and dried in an oven at 110 °C for 24 h; then they have been calcined at 575 °C for 2 h following a temperature ramp of 5 °C·min^{-1} and sieved to a particle diameter between 0.125 and 0.3 mm. This calcination temperature assures the hydrothermal stability of the acid sites that is required for operating in reaction–regeneration cycles (with regeneration by coke combustion with air at 550 °C), with full recovery of the kinetic performance [54]. Additionally, this agglomeration confers a suitable particle size for its use in the reactor. Moreover, the binder and the inert charge provide a matrix with a meso- and macroporous structure embedding the zeolite crystals, which contributes to: (i) improving accessibility of the reaction medium compounds to the zeolite crystals; (ii) facilitating the deposition of coke in the mesoporous matrix, and (iii) favoring heat dissipation in the particle during the regeneration step by coke combustion, thus increasing the hydrothermal stability [30,55].

3.2. Catalyst Characterization

The physical or textural properties of the catalyst (i.e., BET surface area, micropore volume, pore volume, pore size distribution and pore diameter average) were measured using a Micromeritics ASAP 2010 (Norcross, GA, USA), these properties are determined by adsorption-desorption of N_2 (micropore and mesopore formation).

The number of acid sites and the acid strength distribution have been determined by monitoring the adsorption-desorption of tert-butyl amine (t-BA), by combining the techniques of thermogravimetric analysis and differential scanning calorimetry during the adsorption of the base at 100 °C. The amount of acid sites has been quantified as the amount of base chemisorbed at 100 °C, in $mmol_{t\text{-}BA} \cdot g^{-1}$, whereas the acid strength has been defined as the heat released during the adsorption of the base, $kJ \cdot mmol_{t\text{-}BA}{}^{-1}$. Catalyst saturation at 100 °C was followed by temperature-programmed desorption/cracking of t-BA (TPD-cracking) (5 °C·min^{-1} up to 500 °C) using a Setaram TG-DSC (Caluire-et-Cuire, France) calorimeter connected online with a Thermostar mass spectrometer from Balzers Instruments (Berlin, Germany). Above 100 °C, t-BA is cracked on the acid sites releasing butene, whose signal (m/e = 56) is monitored in a mass spectrometer, thereby identifying those sites with enough acidity for cracking t-BA.

3.3. Reaction and Analysis Equipment

The reactions have been performed in an automated stainless steel fixed bed reactor (Microactivity, PID Eng & Tech., Madrid, Spain), with an internal diameter of 9 mm and 10 cm long. The bed consists of a mixture of catalyst and inert particles (silicon carbide). The reactions were carried out feeding pure DME (18 mL·min^{-1}) at temperature of 325–375 °C, pressure of 1.5 atm, space times of 4 $g \cdot h \cdot mol_C{}^{-1}$, during 18 h. A reaction co-feeding water has been carried out using a molar ratio H_2O/DME 3.55 [56]. Prior to the reaction, the transformation of DME (very sensitive to the presence of water) requires an in situ conditioning treatment of the catalyst (at 550 °C with air for 2 h) in order to eliminate the water adsorbed in the acid sites of the catalyst. Reaction products have been analyzed in a micro gas

chromatograph Agilent CP-490 (Santa Clara, CA, USA). The quantification and identification of the compounds has been carried out based on calibration standards of known concentration. Conversion of DME (X) and selectivity (S_i) of each product have been defined as follows:

$$X = \sum F_{products} / F_{total} \quad (1)$$

$$S_i = F_i / \sum F_{products} \quad (2)$$

where $\sum F_{products}$ is the molar flow-rate of the products formed, F_{total} is the total molar flow-rate in the reaction medium and F_i is the molar flow of the product i. These flows are quantified in units of carbon content.

The products obtained are grouped in the following lumps: CO, CO_2, methane, ethylene, propylene, butenes, aromatic compounds or BTX (benzene, toluene and xylene), C_{4-} paraffins and C_{5+} aliphatics.

3.4. Deactivated Catalyst Characterization

The content of carbonaceous species in the deactivated catalysts was calculated with a TGA Q5000TA thermobalance (Thermo Scientific-TA Instruments, New Castle, DE, USA) following the procedure: (1) temperature-programmed desorption (TPD) with N_2 up to 550 °C; (2) temperature-programmed oxidation/combustion (TPO) with air up to 550 °C with a temperature ramp of 5 °C·min^{-1} followed by 90 min of isothermal conditions (to ensure complete combustion of coke); (3) the sample is cooled with a ramp of 15 °C·min^{-1} to 250 °C.

The nature of carbonaceous species has been determined by FTIR spectroscopy on a Nicolet 6700 spectrophotometer (Thermo, Midland, ON, Canada). The deactivated catalyst sample (10 mg) was pelletized with KBr (150 mg, purity > 99%) applying a pressure equivalent to 10 t·cm^{-2}. The sample was degassed at 100 °C for 1 h. Then, air is allowed to pass through the chamber with a flow-rate of 60 mL·min^{-1} and temperature is raised linearly at 5 °C·min^{-1} to 550 °C, maintaining this temperature for 1 h. Simultaneously, the signal of CO_2 (m/z = 44) is recorded on a mass spectrometer (Omni Star, Pfeiffer Vacuum, Assla, Germany).

The UV-Vis absorption measurements were carried out using a Jasco V-780 spectrometer (Easton, MD, USA). The samples were placed on a Scientific Instrument Linkam cell and spectra were collected at different positions along individual catalyst particles and in different catalyst particles, so that the results are averages of these measurements. The absorption measurements were performed in the spectral range of 350–750 nm.

4. Conclusions

The analysis of the deactivated catalysts used in DME conversion evidences that the intermediates involved in the dual cycle mechanism (e.g., alkyl-benzenes) act at the same time as coke precursors; evolving sequentially towards polyalkyl-benzenes and polyaromatic structures. These species are predominantly trapped within the micropores of the zeolite whereas the polyaromatic structures (coke) that lead to the catalyst deactivation are predominantly trapped within the matrix material. Indeed, there is a strong correlation between the nature and location of carbonaceous species in the catalyst: more condensed aromatics in the meso- and macropores of the catalyst (matrix) and less condensed alkyl-benzenes in the micropores.

In order to favor the production of olefins and attenuate the condensation of coke, the properties of the catalyst and the reaction condition must be considered. The presence of a meso- and macroporous matrix (using boehmite as a binder) and steam in the reaction medium favor the sweeping of the coke precursors outside the microporous of the zeolite. The condensation of the polyalkyl-benzenes into bulkier polyaromatics on the matrix surface mitigates the zeolite pores blockage and lengthens the lifetime of the catalyst.

Acknowledgments: The financial support of this work was undertaken by the Ministry of Economy and Competitiveness of the Spanish Government, some cofounded with ERDF funds (Project CTQ2013-46172-P, CTQ2013-46173-R and CTQ2016-79646-P projects), by the Basque Government (Project IT748-13) and by the University of the Basque Country (UFI 11/39). M. Ibáñez is grateful for the postgraduate grant from the University of the Basque Country (No. UPV/EHU2016).

Author Contributions: M.I., P.P.-U. and M.S.-C. were responsible of the experiments; A.T.A. and P.C. were responsible of the experimental design; T.C.-L. wrote parts of the introduction and results, while participating in certain interpretations (Figure 5); M.I., T.C.-L., J.B. and P.C. were responsible of the writing; and P.C. coordinated the work.

Conflicts of Interest: The authors declare no conflict of interest. The founding sponsors had no role in the design of the study; in the collection, analyses, or interpretation of data; in the writing of the manuscript, and in the decision to publish the results.

References

1. Park, Y.K.; Lee, C.W.; Kang, N.Y.; Choi, W.C.; Choi, S.; Oh, S.H.; Park, D.S. Catalytic cracking of lower-valued hydrocarbons for producing light olefins. *Catal. Surv. Asia* **2010**, *14*, 75–84. [CrossRef]
2. Park, S.; Inagaki, S.; Kubota, Y. Selective formation of light olefins from dimethyl ether over MCM-68 modified with phosphate species. *Catal. Today* **2016**, *265*, 218–224. [CrossRef]
3. Sadrameli, S.M. Thermal/catalytic cracking of liquid hydrocarbons for the production of olefins: A state-of-the-art review II: Catalytic cracking review. *Fuel* **2016**, *173*, 285–297. [CrossRef]
4. Chang, C.D.; Chu, C.T.W.; Socha, R.F. Methanol conversion to olefins over ZSM-5. I. Effect of temperature and zeolite SiO_2/Al_2O_3. *J. Catal.* **1984**, *86*, 289–296. [CrossRef]
5. Ateka, A.; Pérez-Uriarte, P.; Gamero, M.; Ereña, J.; Aguayo, A.T.; Bilbao, J. A comparative thermodynamic study on the CO_2 conversion in the synthesis of methanol and of DME. *Energy* **2017**, *120*, 796–804. [CrossRef]
6. Olah, G.A.; Goeppert, A.; Prakash, G.K.S. Chemical recycling of carbon dioxide to methanol and dimethyl ether: From greenhouse gas to renewable, environmentally carbon neutral fuels and synthetic hydrocarbons. *J. Org. Chem.* **2009**, *74*, 487–498. [CrossRef] [PubMed]
7. Ghavipour, M.; Behbahani, R.M.; Rostami, R.B.; Lemraski, A.S. Methanol/dimethyl ether to light olefins over SAPO-34: Comprehensive comparison of the products distribution and catalyst performance. *J. Nat. Gas Sci. Eng.* **2014**, *21*, 532–539. [CrossRef]
8. Olsbye, U.; Svelle, S.; Bjørgen, M.; Beato, P.; Janssens, T.V.W.; Joensen, F.; Bordiga, S.; Lillerud, K.P. Conversion of methanol to hydrocarbons: How zeolite cavity and pore size controls product selectivity. *Angew. Chem.* **2012**, *51*, 5810–5831. [CrossRef] [PubMed]
9. Abasov, S.I.; Babayeva, F.A.; Guliyev, B.B.; Piriyev, N.N.; Rustamov, M.I. Features of methanol and dimethyl ether conversion to hydrocarbons on modified zeolites Y and ZSM-5. *Theor. Exp. Chem.* **2013**, *49*, 58–64. [CrossRef]
10. Pérez-Uriarte, P.; Ateka, A.; Aguayo, A.T.; Bilbao, J. Comparison of HZSM-5 zeolite and SAPO (-18 and -34) based catalysts for the production of light olefins from DME. *Catal. Lett.* **2016**, *146*, 1892–1902. [CrossRef]
11. Hirota, Y.; Yamada, M.; Uchida, Y.; Sakamoto, Y.; Yokoi, T.; Nishiyama, N. Synthesis of SAPO-18 with low acidic strength and its application in conversion of dimethylether to olefins. *Microporous Mesoporous Mater.* **2016**, *232*, 65–69. [CrossRef]
12. Zhao, D.; Zhang, Y.; Li, Z.; Wang, Y.; Yu, J. Synthesis of SAPO-18/34 intergrowth zeolites and their enhanced stability for dimethyl ether to olefins. *RSC Adv.* **2017**, *7*, 939–946. [CrossRef]
13. Zhao, D.; Zhang, Y.; Peng, Y.; Yu, J. A novel preparation of SAPO-18 molecular sieve with enhanced stability for dimethyl ether to olefins. *Catal. Lett.* **2016**, *146*, 2261–2267. [CrossRef]
14. Al-Dughaither, A.S.; De Lasa, H. HZSM-5 zeolites with different SiO_2/Al_2O_3 ratios. Characterization and NH_3 desorption kinetics. *Ind. Eng. Chem. Res.* **2014**, *53*, 15303–15316. [CrossRef]
15. Pérez-Uriarte, P.; Gamero, M.; Ateka, A.; Díaz, M.; Aguayo, A.T.; Bilbao, J. Effect of the acidity of HZSM-5 zeolite and the binder in the DME transformation to olefins. *Ind. Eng. Chem. Res.* **2016**, *55*, 1513–1521. [CrossRef]
16. Al-Dughaither, A.S.; De Lasa, H. Neat dimethyl ether conversion to olefins (DTO) over HZSM-5: Effect of SiO_2/Al_2O_3 on porosity, surface chemistry, and reactivity. *Fuel* **2014**, *138*, 52–64. [CrossRef]

17. Bleken, F.; Skistad, W.; Barbera, K.; Kustova, M.; Bordiga, S.; Beato, P.; Lillerud, K.P.; Svelle, S.; Olsbye, U. Conversion of methanol over 10-ring zeolites with differing volumes at channel intersections: Comparison of TNU-9, IM-5, ZSM-11 and ZSM-5. *Phys. Chem. Chem. Phys.* **2011**, *13*, 2539–2549. [CrossRef] [PubMed]
18. Gil-Coba, J.; Marie-Rose, S.C.; Lavoie, J.M. Effect of water content and catalysts acidity in the products distribution during propylene synthesis with a mixture of DME and methanol. *Catal. Lett.* **2016**, *146*, 2534–2542. [CrossRef]
19. Ilias, S.; Bhan, A. Mechanism of the catalytic conversion of methanol to hydrocarbons. *ACS Catal.* **2013**, *3*, 18–31. [CrossRef]
20. Khare, R.; Liu, Z.; Han, Y.; Bhan, A. A mechanistic basis for the effect of aluminum content on ethene selectivity in methanol-to-hydrocarbons conversion on HZSM-5. *J. Catal.* **2017**, *348*, 300–305. [CrossRef]
21. Liang, T.; Chen, J.; Qin, Z.; Li, J.; Wang, P.; Wang, S.; Wang, G.; Dong, M.; Fan, W.; Wang, J. Conversion of methanol to olefins over H-ZSM-5 zeolite: Reaction pathway is related to the framework aluminum siting. *ACS Catal.* **2016**, *6*, 7311–7325. [CrossRef]
22. Tian, P.; Wei, Y.; Ye, M.; Liu, Z. Methanol to olefins (MTO): From fundamentals to commercialization. *ACS Catal.* **2015**, *5*, 1922–1938. [CrossRef]
23. Hao, J.; Zhao, Y.; Ye, M.; Liu, Z. Influence of temperature on fluidized-bed catalyst attrition behavior. *Chem. Eng. Technol.* **2016**, *39*, 927–934. [CrossRef]
24. Vu, X.H.; Armbruster, U.; Martin, A. Micro/mesoporous zeolitic composites: Recent developments in synthesis and catalytic applications. *Catalysts* **2016**, *6*, 183. [CrossRef]
25. Michels, N.L.; Mitchell, S.; Pérez-Ramírez, J. Effects of binders on the performance of shaped hierarchical MFI zeolites in methanol-to-hydrocarbons. *ACS Catal.* **2014**, *4*, 2409–2417. [CrossRef]
26. Ibáñez, M.; Artetxe, M.; López, G.; Elordi, G.; Bilbao, J.; Olazar, M.; Castaño, P. Identification of the coke deposited on an HZSM-5 zeolite catalyst during the sequenced pyrolysis-cracking of HDPE. *Appl. Catal. B* **2014**, *148*, 436–445. [CrossRef]
27. Guisnet, M.; Magnoux, P. Organic chemistry of coke formation. *Appl. Catal. A Gen.* **2001**, *212*, 83–96. [CrossRef]
28. Schulz, H. "Coking" of zeolites during methanol conversion: Basic reactions of the MTO-, MTP- and MTG processes. *Catal. Today* **2010**, *154*, 183–194. [CrossRef]
29. Olsbye, U.; Svelle, S.; Lillerud, K.P.; Wei, Z.H.; Chen, Y.Y.; Li, J.F.; Wang, J.G.; Fan, W.B. The formation and degradation of active species during methanol conversion over protonated zeotype catalysts. *Chem. Soc. Rev.* **2015**, *44*, 7155–7176. [CrossRef] [PubMed]
30. Castaño, P.; Ruiz-Martinez, J.; Epelde, E.; Gayubo, A.G.; Weckhuysen, B.M. Spatial distribution of zeolite ZSM-5 within catalyst bodies affects selectivity and stability of methanol-to-hydrocarbons conversion. *ChemCatChem* **2013**, *5*, 2827–2831. [CrossRef]
31. Castaño, P.; Elordi, G.; Olazar, M.; Bilbao, J. Imaging the profiles of deactivating species on the catalyst used for the cracking of waste polyethylene by combined microscopies. *ChemCatChem* **2012**, *4*, 631–635. [CrossRef]
32. Aguayo, A.T.; Castaño, P.; Mier, D.; Gayubo, A.G.; Olazar, M.; Bilbao, J. Effect of cofeeding butane with methanol on the deactivation by coke of a HZSM-5 zeolite catalyst. *Ind. Eng. Chem. Res.* **2011**, *50*, 9980–9988. [CrossRef]
33. Gayubo, A.G.; Alonso, A.; Valle, B.; Aguayo, A.T.; Olazar, M.; Bilbao, J. Kinetic modelling for the transformation of bioethanol into olefins on a hydrothermally stable Ni-HZSM-5 catalyst considering the deactivation by coke. *Chem. Eng. J.* **2011**, *167*, 262–277. [CrossRef]
34. Corma, A.; Melo, F.V.; Sauvanaud, L. Attempts to improve the product slate quality: Influence of coke-on-catalyst content. *Ind. Eng. Chem. Res.* **2007**, *46*, 4100–4109. [CrossRef]
35. Epelde, E.; Santos, J.I.; Florian, P.; Aguayo, A.T.; Gayubo, A.G.; Bilbao, J.; Castaño, P. Controlling coke deactivation and cracking selectivity of MFI zeolite by H_3PO_4 or KOH modification. *Appl. Catal. A Gen.* **2015**, *505*, 105–115. [CrossRef]
36. Epelde, E.; Ibañez, M.; Aguayo, A.T.; Gayubo, A.G.; Bilbao, J.; Castaño, P. Differences among the deactivation pathway of HZSM-5 zeolite and SAPO-34 in the transformation of ethylene or 1-butene to propylene. *Microporous Mesoporous Mater.* **2014**, *195*, 284–293. [CrossRef]
37. Epelde, E.; Gayubo, A.G.; Olazar, M.; Bilbao, J.; Aguayo, A.T. Modified HZSM-5 zeolites for intensifying propylene production in the transformation of 1-butene. *Chem. Eng. J.* **2014**, *251*, 80–91. [CrossRef]

38. Gayubo, A.G.; Aguayo, A.T.; Morán, A.L.; Olazar, M.; Bilbao, J. Role of water in the kinetic modeling of catalyst deactivation in the MTG process. *AIChE J.* **2002**, *48*, 1561–1571. [CrossRef]
39. Aguayo, A.T.; Gayubo, A.G.; Atutxa, A.; Olazar, M.; Bilbao, J. Catalyst deactivation by coke in the transformation of aqueous ethanol into hydrocarbons. Kinetic modeling and acidity deterioration of the catalyst. *Ind. Eng. Chem. Res.* **2002**, *41*, 4216–4224. [CrossRef]
40. Mier, D.; Gayubo, A.G.; Aguayo, A.T.; Olazar, M.; Bilbao, J. Olefin production by cofeeding methanol and n-butane: Kinetic modeling considering the deactivation of HZSM-5 zeolite. *AIChE J.* **2011**, *57*, 2841–2853. [CrossRef]
41. Chen, S.; Manos, G. Study of coke and coke precursors during catalytic cracking of n-hexane and 1-hexene over ultrastable y zeolite. *Catal. Lett.* **2004**, *96*, 195–200. [CrossRef]
42. Chen, S.; Manos, G. In situ thermogravimetric study of coke formation during catalytic cracking of normal hexane and 1-hexene over ultrastable y zeolite. *J. Catal.* **2004**, *226*, 343–350. [CrossRef]
43. Bauer, F.; Karge, H.G. Characterization of coke on zeolites. *Mol. Sieves* **2007**, *5*, 249–364.
44. Ibáñez, M.; Gamero, M.; Ruiz-Martínez, J.; Weckhuysen, B.M.; Aguayo, A.T.; Bilbao, J.; Castaño, P. Simultaneous coking and dealumination of zeolite H-ZSM-5 during the transformation of chloromethane into olefins. *Catal. Sci. Technol.* **2016**, *6*, 296–306. [CrossRef]
45. Pérez-Uriarte, P.; Ateka, A.; Gayubo, A.G.; Cordero-Lanzac, T.; Aguayo, A.T.; Bilbao, J. Deactivation kinetics for the conversion of dimethyl ether to olefins over a HZSM-5 zeolite catalyst. *Chem. Eng. J.* **2017**, *311*, 367–377. [CrossRef]
46. Mukarakate, C.; McBrayer, J.D.; Evans, T.J.; Budhi, S.; Robichaud, D.J.; Iisa, K.; Ten Dam, J.; Watson, M.J.; Baldwin, R.M.; Nimlos, M.R. Catalytic fast pyrolysis of biomass: The reactions of water and aromatic intermediates produces phenols. *Green Chem.* **2015**, *17*, 4217–4227. [CrossRef]
47. Pérez-Uriarte, P.; Ateka, A.; Aguayo, A.T.; Gayubo, A.G.; Bilbao, J. Kinetic model for the reaction of DME to olefins over a HZSM-5 zeolite catalyst. *Chem. Eng. J.* **2016**, *302*, 801–810. [CrossRef]
48. Karge, H.G.; Nießen, W.; Bludau, H. In-situ FTIR measurements of diffusion in coking zeolite catalysts. *Appl. Catal. A Gen.* **1996**, *146*, 339–349. [CrossRef]
49. Arsenova, N.; Bludau, H.; Haag, W.O.; Karge, H.G. In situ IR spectroscopic study of the adsorption behaviour of ethylbenzene and diethylbenzenes related to ethylbenzene disproportionation over hy zeolite. *Microporous Mesoporous Mater.* **1998**, *23*, 1–10. [CrossRef]
50. Castaño, P.; Elordi, G.; Olazar, M.; Aguayo, A.T.; Pawelec, B.; Bilbao, J. Insights into the coke deposited on HZSM-5, Hβ and HY zeolites during the cracking of polyethylene. *Appl. Catal. B Environ.* **2011**, *104*, 91–100. [CrossRef]
51. Aguayo, A.T.; Gayubo, A.G.; Ereña, J.; Atutxa, A.; Bilbao, J. Coke aging and its incidence on catalyst regeneration. *Ind. Eng. Chem. Res.* **2003**, *42*, 3914–3921. [CrossRef]
52. Mores, D.; Stavitski, E.; Kox, M.H.F.; Kornatowski, J.; Olsbye, U.; Weckhuysen, B.M. Space- and time-resolved in-situ spectroscopy on the coke formation in molecular sieves: Methanol-to-olefin conversion over H-ZSM-5 and H-SAPO-34. *Chem. Eur. J.* **2008**, *14*, 11320–11327. [CrossRef] [PubMed]
53. Mores, D.; Kornatowski, J.; Olsbye, U.; Weckhuysen, B.M. Coke formation during the methanol-to-olefin conversion: In situ microspectroscopy on individual H-ZSM-5 crystals with different brønsted acidity. *Chem. A Eur. J.* **2011**, *17*, 2874–2884. [CrossRef] [PubMed]
54. Benito, P.L.; Aguayo, A.T.; Gayubo, A.G.; Bilbao, J. Catalyst equilibration for transformation of methanol into hydrocarbons by reaction-regeneration cycles. *Ind. Eng. Chem. Res.* **1996**, *35*, 2177–2182. [CrossRef]
55. Aguayo, A.T.; Gayubo, A.G.; Vivanco, R.; Olazar, M.; Bilbao, J. Role of acidity and microporous structure in alternative catalysts for the transformation of methanol into olefins. *Appl. Catal. A Gen.* **2005**, *283*, 197–207. [CrossRef]
56. Pérez-Uriarte, P.; Ateka, A.; Gamero, M.; Aguayo, A.T.; Bilbao, J. Effect of the operating conditions in the transformation of DME to olefins over a HZSM-5 zeolite catalyst. *Ind. Eng. Chem. Res.* **2016**, *55*, 6569–6578. [CrossRef]